# Compensation of Parasitic Effect in Homing Loop with Strapdown Seeker via PID Control

Ju-Hyeon Hong and Chang-Kyung Ryoo
*Department of Aerospace Engineering, Inha University, Inharo100, Incheon, Korea*

Keywords: Homing Loop, Strapdown Seeker, Parasitic Effect, PID Controller.

Abstract: Due to seeker delay and coupling with body motion, a strapdown seeker has not been widely used for missiles though it makes the missile cost cheaper. In this paper, a homing loop design based on PID controller for missiles with a strapdown seeker is suggested. The PID controller produces body rate command, instead of estimating line-of-sight(LOS) rate for the proportional navigation guidance. Stability analysis for linear homing loop has been done to select controller gains. The performance of the designed terminal homing loop for a small tactical missile against a moving target, where the missile's strapdown seeker includes uncertain image processing delay, is verified through full nonlinear 6-DOF simulations.



## 1 INTRODUCTION

Strapdown seekers have many advantages compared to gimballed seekers. They are small and light, requiring less power, and most of all low cost for production. However, the field of view(FOV) of a strapdown seeker is narrow and its look angle measurements are severely correlated with body motion. Because the strapdown seeker is fixed on body of missile, it only measures a look angle, the angle between body axis and the LOS. Hence, to implement widely used proportional navigation(PN) guidance, some signal processing techniques to obtain the LOS rate are required (Ozkan, 2005). Theoretically, the LOS rate can be calculated via subtracting the body attitude rate simply from the look angle rate in which the LOS rate is implicitly included. Typically, the body attitude rate is measured from a rate gyro, while the look angle rate is obtained by a numerical filter differentiating the look angle measured from the seeker. The look angle measurements from the seeker are delayed due to target image processing and tracking when it compared to the body rate from the rate gyro. Due to the seeker delay, the body attitude rate implicitly imbedded in the look angle rate cannot be nullified by the body attitude rate measured by rate gyro. We call the phenomenon caused by this signal discrepancy the parasitic effect. Different signal characteristics between the look angle rate and the body rate makes the entire missile homing loop unstable.

Several guidance methods have been studied for missiles with the strapdown seeker. The most widely used method is to correct the scale factors which are located at outputs of seeker and rate gyro of the homing loop. The extended Kalman filter(EKF) has been used to estimate scale factor (Mehra, and Ehrich, 1984). It is reported that the scale factor uncertainty breaks down the optimality of guidance (Willman, 1988). The linear quadratic Gaussian (LQG) method is adopted to replace PN guidance for missiles with the strapdown seeker where EKF is also used for estimating the state information including scale factor error (Vergez and McClendon, 1982). The stability of the parasitical loop effected by scale factor errors has been analysed (Du, Xia, and Guo, 2010).

While the previous studies mentioned above are related to estimate the scale factors, there have been some tries to estimate LOS rate directly by using the guidance filter for missiles with the strapdown seeker. The unscented Kalman filter (UKF) is used to estimate relative motion of the missile to a target (Yun, Ryoo, and Song, 2009). Instead of estimating the LOS rate, a look angle control method to deliver the missile to a destination has been proposed (Kim, Park, and Ryoo, 2013). This method is very simple for implementation and free from parasitic effect because it does not require any estimation filter. But the missile behaviour under the look angle control is

Hong J. and Ryoo C..
Compensation of Parasitic Effect in Homing Loop with Strapdown Seeker via PID Control.
DOI: 10.5220/0005055907110717
In *Proceedings of the 11th International Conference on Informatics in Control, Automation and Robotics* (ICINCO-2014), pages 711-717
ISBN: 978-989-758-039-0

very similar to that under the pursuit guidance: weak to disturbances and target manoeuvre. To calculate LOS rate, the image plane value method is introduced (Kim, Park, and Lee, 2009). To compensate the signal difference between the body attitude rate and the look angle rate, the known seeker delay is compulsively placed at the rate gyro output (Jang, Ryoo, Choi, and Tahk, 2008). Here, the alpha-beta filter to calculate the LOS rate is used. Routh-Hurwitz stability criterion to select the loop gain has been also introduced to reduce the parasitic effect (Kim, Park, Kwon, Kim, and Tahk, 2011).

In this paper, the PID control method is proposed to stabilize the missile homing loop including the delay of the strapdown seeker. First, we place the pure seeker delay on the output of the rate gyro. In this way, the time difference between the seeker signal and rate gyro signal is removed. Then, LOS angle is calculated by subtracting the body attitude angle which is obtained by integrating the body attitude rate from the look angle. The PID controller is then designed to produce the guidance command. Stability analysis for the linear homing loop is then done to select PID gains.

In the subsequent section, problems imbedded in the conventional homing loop of missile with the strapdown seeker are addressed. In Section 3, the homing loop design approach based on PID is introduced. Full nonlinear 6-DOF simulations to verify the performance of the proposed approach is performed in Section 4. Section 5 is concluding remarks.

## 2 PROBLEM DEFINITION

### 2.1 Missile Model and Angular Guidance Command

We consider in this paper that the missile only have a strapdown seeker and a 3-axis gyroscope. This kind of sensor suites is adequate for a low cost small tactical missile whose target is likely light armoured vehicles and bunkers within the range of 1.5km.

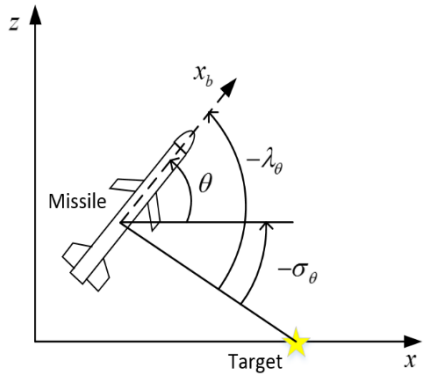

Figure 1: Guidance geometry in the pitch channel.

In this paper, we assume that roll is tightly stabilized, and pitch and yaw channel are independent each other. The guidance geometry at pitch channel is illustrated on Figure 1.

The LOS angle $\sigma$ is the sum of the body attitude angle and the look angle. The guidance geometry in the yaw channel has the same as that of pitch channel. The equations of the LOS angles in the pitch channel and the yaw channel are respectively given by

$$\begin{aligned} \sigma_\theta &= \lambda_\theta + \theta \\ \sigma_\psi &= \lambda_\psi + \psi \end{aligned} \tag{1}$$

where $\lambda_\theta$ and $\lambda_\psi$ are look angles, respectively and they are measured by the strapdown seeker. The body pitch and yaw angles are denoted by $\theta$ and $\psi$, respectively.

The acceleration commands along with the pitch and yaw axes are respectively given by $a_{x_c}$ and $a_{z_c}$. In case of the proportional navigation guidance, the guidance commands are given by.

$$\begin{aligned} a_{x_\sigma} &= NV_m\dot{\sigma}_\theta + g \\ a_{y_\sigma} &= NV_m\dot{\sigma}_\psi \end{aligned} \tag{2}$$

where $N$ the guidance coefficient, $V_m$ the missile velocity, and $g$ the gravitational acceleration. The LOS angular rate $\dot{\sigma}$ in the pitch and yaw channels is derived by the sum of the body angular rate and the look angle rate ( $\dot{\lambda}$ ).

$$\begin{aligned} \dot{\sigma}_\theta &= q + \dot{\lambda}_\theta \\ \dot{\sigma}_\psi &= r + \dot{\lambda}_\psi \end{aligned} \tag{3}$$

where $q$ and $r$ are the pitch and yaw angular rate, respectively. Since the missile has axis gyroscopes so that the guidance acceleration command must be converted into the body angular rate command as follows.

$$\begin{aligned} q_c &= N\dot{\sigma}_\theta + \frac{g}{V_m} \\ r_c &= N\dot{\sigma}_\psi \end{aligned} \tag{4}$$

where $q_c$ and $r_c$ denote the pitch and yaw angular rate commands, respectively. Since the speed of missile cannot be measured, the average speed estimated from simulations is applied to compensate gravity in (4).

## 2.2 Ideal Homing Loop

Figure 2 shows the ideal PN homing loop in the pitch channel for a missile with a strapdown seeker. Here, the LOS rate $\dot{\sigma}$ for PN is produced by the sum of the pitch body rate $q$ and the look angle rate $\dot{\lambda}$. While $q$ is measured by the rate gyro, $\dot{\lambda}$ is given by the derivative of the seeker look angle $\lambda$. Realizable homing loop is given in Figure 3, where the derivative term in Figure 2 is replaced by $\alpha-\beta$ filter.

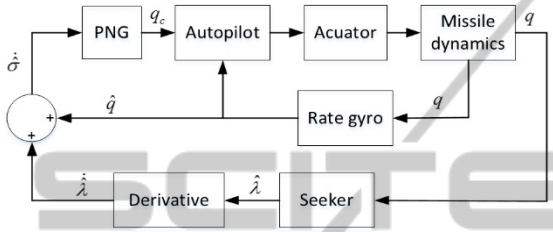


Figure 2: Pitch channel ideal homing loop for missile with strapdown seeker.

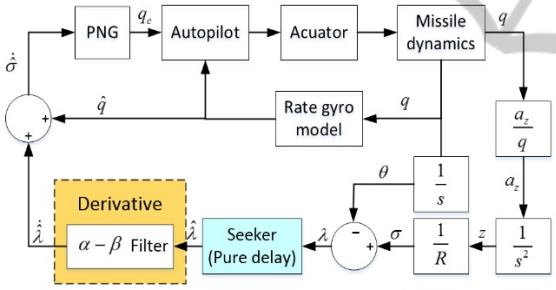


Figure 3: Original homing loop.

### 2.2.1 Linear Modelling of Time Delay

In order for analysis of homing loop, the time delay of the seeker and the sampling time are modelled as

$$G(s)=e^{-sT} \tag{5}$$

$$H(z)=z^{-T/\Delta T} \tag{6}$$

where $T$ and $\Delta T$ denote the time delay time and the sampling time, respectively. Pade approximation is used to transform the exponential function in (5) into rational transfer function (Dorf, and Bishop, 2008).

### 2.2.2 Design of $\alpha-\beta$ Filter (Kalata, 1984)

The $\alpha-\beta$ filter can be used for obtaining the look angle rate (Jang, Ryoo, Choi, and Tahk, 2008). The state vector is defined by

$$x(k)=\left[\lambda(k)\quad \dot{\lambda}(k)\right]^T. \tag{7}$$

The system equation and measurement equation are given by

$$x(k+1)=\Phi x(k)+\Psi w(k) \tag{8}$$

$$\Phi=\begin{bmatrix}1 & \Delta T\\ 0 & 1\end{bmatrix},\Psi=\begin{bmatrix}0.5\Delta T^2\\ \Delta T\end{bmatrix},w(k)\sim N(0,Q) \tag{9}$$

$$y(k)=hx(k)+n(k) \tag{10}$$

$$h=\begin{bmatrix}1 & 0\end{bmatrix}^T,n(k)\sim N(0,R) \tag{11}$$

The equations for propagation and updating the state vector are given by

$$\hat{x}(k+1\,|\,k)=\Phi\hat{x}(k\,|\,k) \tag{12}$$

$$\begin{aligned}\hat{x}(k+1\,|\,k+1)&=\hat{x}(k+1\,|\,k)\\&+K(k+1)\left[y(k+1)-h\hat{x}(k+1\,|\,k)\right]\end{aligned} \tag{13}$$

$$K=\begin{bmatrix}\alpha & \beta/\Delta T\end{bmatrix}^T \tag{14}$$

Based on (12)-(14), the $\alpha-\beta$ filter to estimate look angle rate is given by

$$\begin{aligned}\hat{\lambda}(k)&=\hat{\lambda}(k-1)+\Delta T\dot{\hat{\lambda}}(k-1)\\&+\alpha(k)\left[\lambda(k)-\hat{\lambda}(k-1)-\Delta T\dot{\hat{\lambda}}(k-1)\right]\end{aligned} \tag{15}$$

$$\begin{aligned}\dot{\hat{\lambda}}(k)&=\dot{\hat{\lambda}}(k-1)\\&+\frac{\beta(k)}{\Delta T}\left[\lambda(k)-\hat{\lambda}(k-1)-\Delta T\dot{\hat{\lambda}}(k-1)\right]\end{aligned} \tag{16}$$

The filter gains $\alpha,\beta$ are determined by the functions of the process and measurement noise covariances, respectively denoted by $\sigma_w$ and $\sigma_n$.

$$\beta=\frac{\Lambda}{4}\left(\Lambda+4-\sqrt{\Lambda^2+8\Lambda}\right) \tag{17}$$

$$\alpha=1-\frac{\beta^2}{\Lambda^2} \tag{18}$$

$$\Lambda=\frac{T^2\sigma_w}{\sigma_n} \tag{19}$$

### 2.2.3 Transfer Functions of Missile

The transfer functions of the missile for short period pitch motion are given by e

$$\frac{\alpha(s)}{\delta_p(s)}=\frac{Z_\delta s+M_\delta-M_qZ_\delta}{s^2-(Z_\alpha+M_q)s+(Z_\alpha M_q-M_\alpha)} \tag{20}$$

$$\frac{q(s)}{\delta_p(s)}=\frac{M_\delta s+(M_\alpha Z_\delta-Z_\alpha M_\delta)}{s^2-(Z_\alpha+M_q)s+(Z_\alpha M_q-M_\alpha)} \tag{21}$$

where $Z_\alpha$, $M_\alpha$, $M_q$, $Z_\delta$, $M_\delta$ are the dimensional aerodynamic and control derivatives. The transfer function of the actuator is assumed by 1. And the transfer function of the pitch rate response to the pitch rate command, which is based the PI controller, is given by the following equation

$$\frac{q(s)}{q_c(s)} = \frac{K_{qt}K_q\left[M_\delta s + (M_\alpha Z_\delta - Z_\alpha M_\delta)\right]}{s^2 + 2\zeta_q\omega_q s + \omega_q^2} \quad (22)$$

$$2\zeta_q\omega_q = K_q M_\delta - Z_\alpha - M_q$$
$$\omega_q^2 = Z_\alpha M_q - M_\alpha + K_q\left(M_\alpha Z_\delta - Z_\alpha M_\delta\right) \quad (23)$$

where $\zeta_q$ and $\omega_q$ are the damping coefficient and the natural frequency, which are the design objectives of the PI controller. Using (23), we can select the controller gains of $K_q$, $K_{qt}$ to satisfy $\zeta_q$ and $\omega_q$.

The gyroscope model is assumed by the second order system.

$$G_{gyro}(s) = \frac{\omega_n^2}{s^2 - s\zeta\omega_n + \omega_n^2} \quad (24)$$

The stability of the linear homing loop given in Figure 3 with the block components described in the previous section can be done. Note that $\theta$, the pitch attitude, passes through the block components of the pure delay and the $\alpha-\beta$ filter. It means the signal $\dot{\hat{\lambda}}$ implicitly includes the pitch attitude rate. By adding $\hat{q}$ to $\dot{\hat{\lambda}}$, we hope to obtain the LOS rate $\dot{\hat{\sigma}}$. However, the both pitch rate signals are not compensated each other. It implies that $\dot{\hat{\sigma}}$ is corrupted by some signals which comes from the discrepancy between the pitch rates signals. This makes the entire homing loop be unstable.

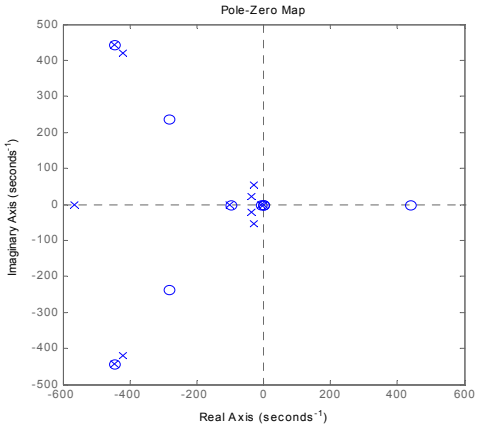


Figure 4: Pole-Zero Map of the original loop.

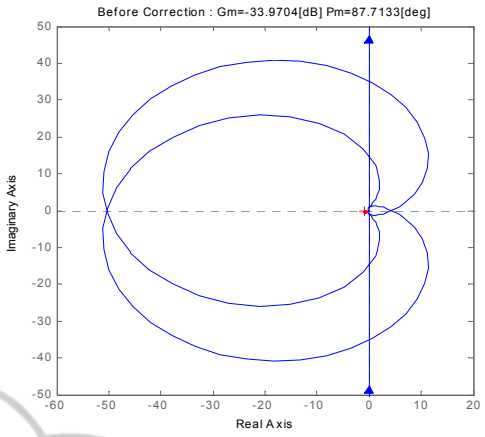


Figure 5: Nyquist diagram of the original loop.

Figure 4 shows open loop pole-zero map of the linear model given in Figure 3. Figure 5 shows Nyquist diagram of this system. Since the number of counter-clockwise encirclements of the (-1, 0) point is two, this linear model is unstable even though there are no poles on the right half plane in Figure 4. This linear model is made up under the condition that relative distance is 1500m and velocity is Mach 0.7.

# 3 HOMING LOOP STABILITY ENHANCEMENT

## 3.1 Homing Loop Performance Improvement through Adding PID Controller

To remedy the parasitic loop effect, we slightly modify the linear homing loop. Instead of introducing the $\alpha-\beta$ filter to estimate the look angle rate, we make the both signals of the gyro and the seeker coincident with each other by adding seeker delay and the $\alpha-\beta$ filter transfer function to the signal loop of the gyro and the gyro transfer function is added to the loop of the seeker as shown in Figure 6. Even we make the two signal loops become coincident with each other by adding some components, there may still signal discrepancies. Hence we add the PID control loop stabilized the homing loop as shown in Figure 6. The PID control loop has the form follows:

$$G_{PID}(s) = K_P + K_I\frac{1}{s} + K_D\frac{K_N s}{s + K_N} \quad (25)$$

Proper choice of gains of PID controller ensures the linear homing loop invent in Figure 6 stable. As mentioned before, we assume the range is fixed with some values to analyse their stability. To ensure the stability for the entire trajectory, we adopt the gain scheduling technique to the guidance loop.

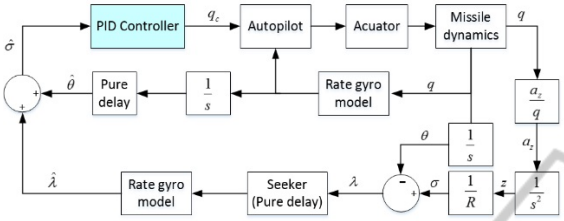


Figure 6: Homing loop with signal compensation and PID controller.

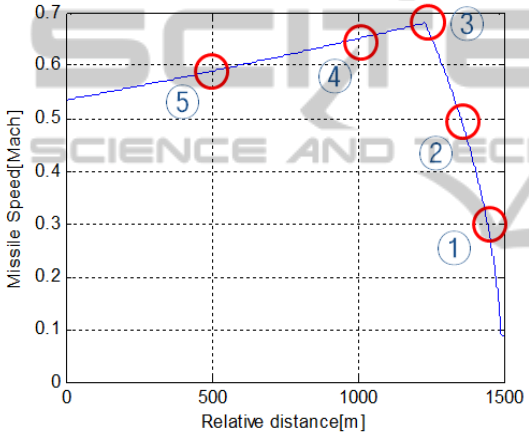


Figure 7: Design point candidates.

We first selected the gain sets of the PID Controller at 5 different missile speeds. Each gain set is then applied to other design points and the stability is checked. Among 5 gain sets, we can choose one gain set that guarantees the stability and performance at all design points. In actual system, we apply this selected gain set to the whole flight condition because the missile speed cannot be measured.

Figure 7 shows the example of design points. The selected design point is the 5th point with the gain margin is 16.2542dB and phase margin is 58.5176deg. When it applied to other design point, the smallest gain and phase margin are 7.51dB and 24.7153deg, respectively.

## 4 SIMULATIONS

Nonlinear 6DOF simulations are performed to analyse the performance of the proposed homing loop. Table 1 shows initial conditions of 6 DOF simulations. The target velocity is 51km/h on horizontal plane.

Figure 8 shows the nonlinear simulation results for the standard conditions with no seeker delay error. In this case, the real seeker delay and the delay compensation for matching signal characteristics are the same with 60msec. We can observe from the figure that the missile states are satisfactorily. Figure 9 and Figure 10 show the nonlinear simulation results with seeker delay error with -20msec and 20msec, respectively. In these cases, the real seeker delay time is 60msec, but the models to compensate the delay in the signal line of rate gyro are 40msec and 80msec, respectively. Except there are small oscillations in the initial phase compared to Figure 8, the missile states are still satisfactorily maintained for both error cases.

Table 1: Initial conditions for 6-DOF simulation.

| | Initial value |
|---|---|
| Initial position of Missile | (0m, 0m, 0m) |
| Initial position of Target | (1500m, 0m, 0m) |
| Initial velocity of Target | (10m/s, 10m/s, 0m/s) |
| Real seeker delay time | 60msec |
| Guidance control loop sampling time | 20msec |

The oscillations in the initial phase are turned out to be within a tolerable range. The guidance errors for the above three simulation cases are in 2m.

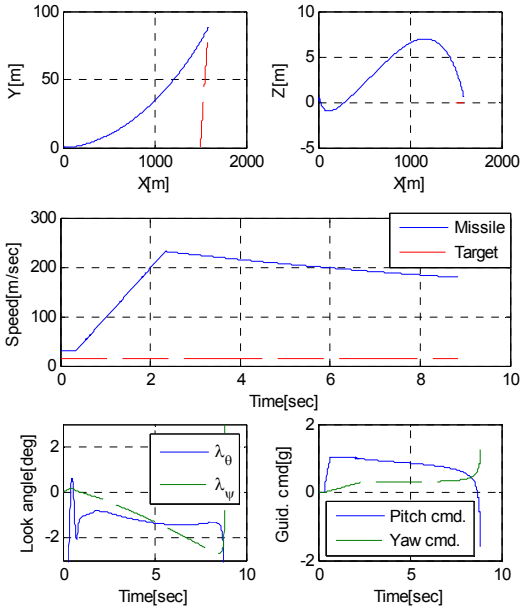


Figure 8: Simulation results without the seeker delay error.

Figure 11 and Figure 12 show the nonlinear simulation results for applying the gain set to the different ranges of 1,000m and 500m, respectively. In these cases, the seeker delay error is not considered. Even though the controller is designed for the target with range of 1,500m, the homing loop is properly working at other target ranges. The guidance error is bounded within 2m.

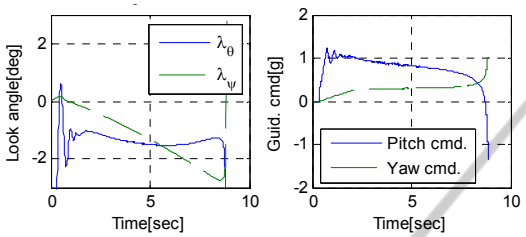


Figure 9: Simulation results for the seeker delay error of d –20msec (40msec pure delay model).

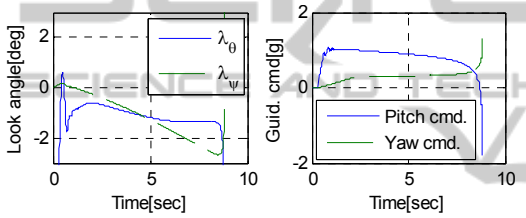


Figure 10: Simulation results for the seeker delay error of +20msec (80msec pure delay model).

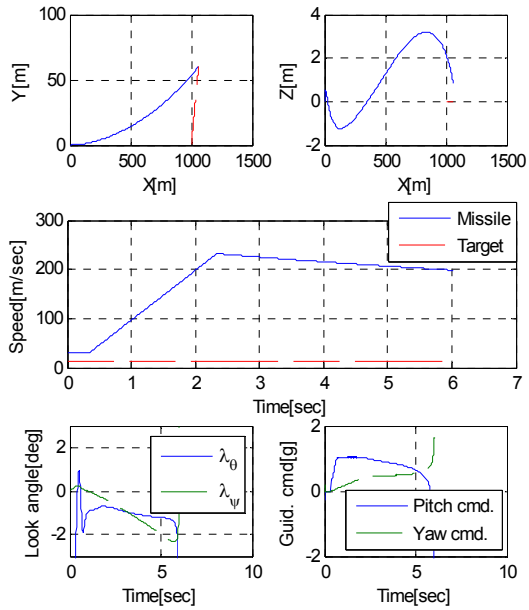


Figure 11: Simulation results for the target range of 1000m.

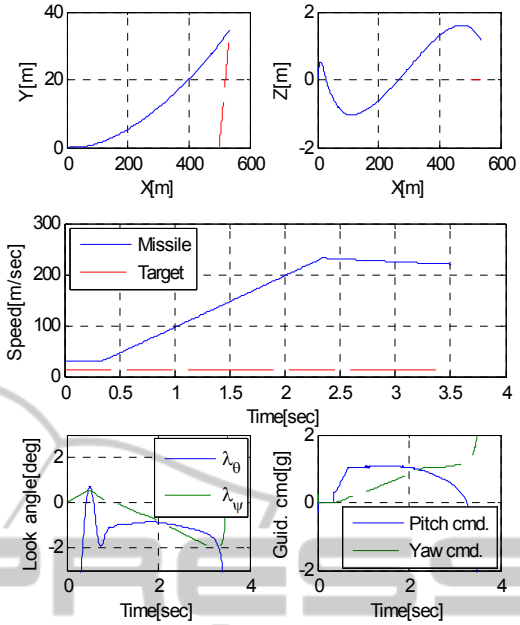


Figure 12: Simulation results for the target range of 500m.

## 5 CONCLUSION

In this paper, the controller design method to compensate the parasitic loop inherently included in the missile homing loop with the strapdown seeker. Method which matches signal characteristic between the seeker delay and the filter dynamics to estimate the look angle rate are the major elements to make the homing loop unstable. Loop consistency via placing the delay and the filter transfer at the output of the rate gyro is considered. Conventional PID control technique is then applied to guarantee the stability of the homing loop against the uncertain seeker delay errors. Thus the proposed method is to nullify the LOS angle instead of the nullifying the LOS rate. Full nonlinear 6-DOF simulations have been done to verify the performance of the proposed method.

## ACKNOWLEDGEMENTS

This study has been done under the support of the Agency for Defence Development in Korea.

## REFERENCES

Ozkan, B., 2005, Dynamic modelling, guidance, and

control of homing missiles. Ph.D Thesis, Middle east technical university, pp. 158-159.

Mehra, R. K., and Ehrich, R. D., 1984, "Air-To-Air Missile Guidance For Strapdown Seekers", *Proceeding of the 23rd Conference on Decision and Control*, Las Vegas, NV, pp.1109-1115.

Willman, W. W., 1988, "Effects of Strapdown Seeker Scale-Factor Uncertainty on Optimal Guidance", *J. Guidance*, VOL.11, NO.3, pp.199-206.

Vergez, P. L., and McClendon, R., 1982, "Optimal Control and Estimation for Strapdown Seeker Guidance of Tactical Missiles", *J. Guidance*, VOL. 5, NO.3, pp.225-226.

Du, Y. L., Xia, Q. L., and Guo, T., 2010,"Study on Stability of Strapdown Seeker Scale Factor Error Parasitical Loop", *Proceeding of 2010 International Conference on Computer, Mechatronics, Control and Electronic Engineering (CMCE)*, VOL. 6, Changchun, Aug., pp.55-58.

Yun, J., Ryoo, C. K., and Song T. L., 2009, "Guidance Filter Design Based on Strapdown Seeker and MEMS Sensors", *Journal of The Korean Society for Aeronautical and Space Sciences*, Vol.37, No.10, pp.1002-1009.

Kim, D., Park, W., and Ryoo, C. K., 2013, "Look-Angle-Control Guidance for Missiles with Strapdown Seeker", *Journal of Institute of Control, Robotics and Systems,* Vol.19, No.3, pp.275-280.

Kim, W. H., Park, C. G., and Lee, J. G., 2009, "A Derivation of LOS Rate for PNG in a Strapdown Seeker Missile", *Proceeding of 2009 the Korea Institute of Military Science and Technology*, Jeju, Korea, pp.354-357.

Jang, S. A., Ryoo, C. K., Choi, K., and Tahk, M. J., 2008, "Guidance Algorithms for Tactical Missiles with Strapdown Seeker ", *Proceeding of SICE Annual Conference 2008*, Tokyo, pp.2616-2619.

Kim T. H, Park, B. G., Kwon, H. H., Kim Y. H., and Tahk, M. J., 2011, "Stability Analysis of Missiles with Strapdown Seeker", *Journal of the Korean Society for Aeronautical and Space Sciences*, Vol.39, No.4, pp.332-340.

Dorf, R. C., and Bishop, R. H., 2008, *Modern Control Systems*, Eleventh edition, Pearson Education, NJ, pp.604-607.

Kalata, P. R., 1984, "The Tracking Index A Generalized Parameter for α-β and α-β-γ Target Trackers", *IEEE Transactions on Aerospace and Electronic Systems*, Volume:AES-20, Issue:2, pp.174-182.